

Probabilistic magnetometry with two-spin system in diamond

Raúl Coto,^{1,*} Hossein T. Dinani,^{1,2} Ariel Norambuena,¹ Mo Chen,³ and Jerónimo R. Maze²

¹*Centro de Investigación DAITA Lab, Facultad de Estudios Interdisciplinarios, Universidad Mayor, Chile*

²*Instituto de Física, Pontificia Universidad Católica de Chile, Casilla 306, Santiago, Chile*

³*Department of Mechanical Engineering, Massachusetts Institute of Technology, 77 Massachusetts Avenue, Cambridge, Massachusetts 02139, USA*

Solid-state magnetometers like the Nitrogen-Vacancy center in diamond have been of paramount importance for the development of quantum sensing with nanoscale spatial resolution. The basic protocol is a Ramsey sequence, that imprints an external static magnetic field into phase of the quantum sensor, which is subsequently readout. In this work we show that the hyperfine coupling between the Nitrogen-Vacancy and a nearby Carbon-13 can be used to set a post-selection protocol that leads to an enhancement of the sensitivity under realistic experimental conditions. We found that for an isotopically purified sample the detection of weak magnetic fields in the μT range can be achieved with a sensitivity of few $\text{nTHz}^{-1/2}$ at cryogenic temperature (4 K), and $0.1 \mu\text{THz}^{-1/2}$ at room temperature.

PACS numbers:

I. INTRODUCTION

Quantum metrology takes advantage of the quantum properties of the system to achieve better precisions than allowed by its classical counterpart [1]. In particular, probabilistic quantum metrology aims to further increase the retrievable information of a parameter by means of a selective measurement. Inspired by the findings of Aharonov, Albert and Vaidman [2], where a measurement sequence consisting of pre-selection, weak measurement and post-selection leads to an anomalous amplification of the measurement result, several theoretical works [3–7] and experiments [8–17] have followed to explore such anomalous amplification. Nevertheless, there remains a longstanding controversy regarding whether probabilistic quantum metrology has practical advantages over standard techniques for parameter estimation [16, 18–23]. In this work, we investigate the important case of spin magnetometry with color centers in diamond, and provide experimental parameter regimes where probabilistic quantum metrology performs better than conventional Ramsey spectroscopy.

Quantum sensors, in particular solid-state magnetometers like the Nitrogen-Vacancy (NV) center in diamond have attracted widespread attention as a powerful tool at the nanoscale [24–32]. Development of sensing protocols and experimental techniques facilitates detection of weak magnetic fields, featuring applications including sensing of single protein [33], small molecules [34], single spins [35, 36], and more recently 3D reconstruction of a nuclear spin cluster [37].

In the following, we focus on DC magnetometry using an NV center. The conventional measurement is realized by a Ramsey sequence with only the electronic spin of NV. Here we consider in addition a weakly cou-

pled ^{13}C nuclear spin located nearby the NV center. We show that by following a particular sequence involving post-selection, one can achieve better magnetic field sensitivity—the minimum detectable magnetic field in a fixed interrogation (sensing) time.

II. THEORY

The original proposal to explore the physics behind weak measurement involves the weak interaction between a qubit and a meter (weak measurement) followed by a post-selection on the qubit state (strong measurement) [2]. A general review could be found in Refs. [3, 6]. In this proposal, Aharonov, Albert and Vaidman considered the meter state expanded in a continuous variable space like the position or momentum space. Their measurement sequence led to an anomalous amplification of the meter observable, which is termed "Weak Value Amplification". This is later generalized to the case where the meter is also a qubit with discrete states [38], which we describe below. Let us consider two spin-1/2 particles interacting through the Hamiltonian $H_i = g\sigma_1^z\sigma_2^z$, with g the coupling strength and σ_1^z (σ_2^z) the \hat{z} -component of Pauli operator acting on the system (meter). First, we prepare the system (meter) in the initial state $|\psi_i\rangle$ ($|\phi_i\rangle$) and let them interact for a certain time t_c , fulfilling $gt_c \ll 1$. After post-selecting the system in the state $|\psi_f\rangle$, the final state of the meter reads (up to renormalization)

$$\begin{aligned} |\phi_f\rangle &= \langle\psi_f|e^{-it_c H_i}|\psi_i\rangle|\phi_i\rangle \\ &\approx \langle\psi_f|\psi_i\rangle(\mathbb{1} -igt_c\langle\sigma_1^z\rangle_w\sigma_2^z)|\phi_i\rangle, \end{aligned} \quad (1)$$

with $\langle\sigma_1^z\rangle_w = \langle\psi_f|\sigma_1^z|\psi_i\rangle/\langle\psi_f|\psi_i\rangle$ being the weak value. The final outcome is the expectation value of the meter

*Electronic address: raul.coto@umayor.cl

operator σ_2^z ,

$$\begin{aligned} \langle \sigma_2^z \rangle &= \frac{\langle \phi_f | \sigma_2^z | \phi_f \rangle}{\langle \phi_f | \phi_f \rangle} \approx \langle \phi_i | \sigma_2^z | \phi_i \rangle \\ &+ 2gt_c \text{Im}[\langle \sigma_1^z \rangle_w] (\langle \phi_i | (\sigma_2^z)^2 | \phi_i \rangle - \langle \phi_i | \sigma_2^z | \phi_i \rangle^2). \end{aligned} \quad (2)$$

The above equation shows that $\langle \sigma_2^z \rangle$ is proportional to the imaginary part of the weak value which can be, in principle, a very large quantity.

Our protocol follows a similar procedure, consisting of pre-selection, weak interaction and post-selection. However, instead of amplifying the weak signal from the qubit-qubit interaction itself, we take advantage of the weak interaction and use it to enhance the sensitivity for an external magnetic field. For convenience, we replace the initial state preparation and final state post-selection by two unitary rotations. The composite system evolves according to $U = R_1(\theta_f)U_\tau R_1(\theta_i)R_2(\alpha)$. Here, the operator $R_1(R_2)$ represents rotations of the system (meter) and U_τ is the free evolution of time τ under the intrinsic Hamiltonian. Hence, the post-selected state will be given by $\rho_{post} = \langle \psi_f | U \rho_i U^\dagger | \psi_f \rangle$, and the expectation value of the meter observable is

$$\langle \sigma_2^z \rangle = \frac{\text{Tr}_2 [\rho_{post} \sigma_2^z]}{\text{Tr}_2 [\rho_{post}]}. \quad (3)$$

We are interested in the narrow shape of the signal $\langle \sigma_2^z \rangle$ that can be obtained by tuning the angles $\{\alpha, \theta_i, \theta_f\}$ and the free evolution time τ . This particular feature will be our starting point to enhance the magnetic field measurement, and it is independent of the fact of having amplification or not. The amplification of the signal and a better sensitivity could be attained in the same protocol. A significant amplification has been observed in a similar system, but with the weak measurement being controlled by a pulse sequence composed of a couple of CNOT gates [15].

In the next section, we will show how this narrow shape of the signal turns out to be beneficial and how this procedure can be implemented in a real quantum nanosensor with current technologies at low temperature. This allows us to implement the protocol performing single-shot readout, improving the signal-to-noise ratio. Moreover, we will discuss the case where the protocol is performed at room temperature and how this affects the performance.

III. THE MODEL

Consider a concrete bi-partite system model given by an electronic spin-1 ($S = 1$) of a negatively charged Nitrogen-Vacancy center (NV^-) and a nearby nuclear spin-1/2 ($I = 1/2$) of a Carbon-13 (^{13}C), as illustrated in Fig. 1-(a).

The ground state of the NV^- is a spin triplet labelled by the spin quantum number $m_s = 0, \pm 1$ ($S = 1$). An

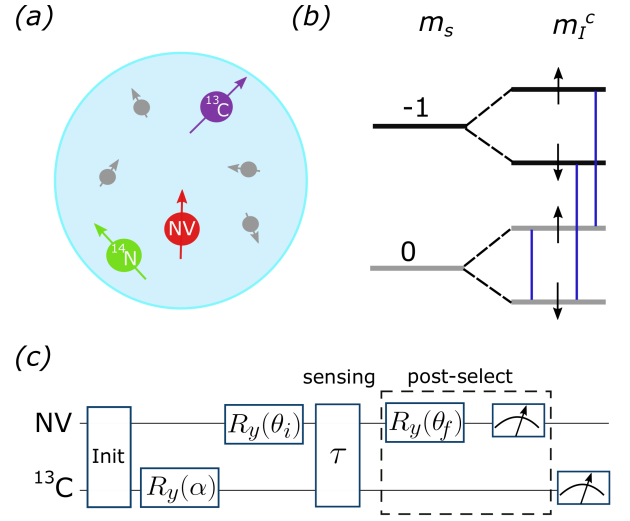


FIG. 1: (a) The electronic spin of a negatively charged NV center interacts with a nuclear spin corresponding to a Carbon-13. (b) Energy levels and relevant transitions. (c) Sequence for both electronic and nuclear spins.

external magnetic field B_z along the N-V axis (z -axis) induces Zeeman energy splitting between the spin sublevels $m_s = +1$ and $m_s = -1$ and lifts their degeneracy. The ^{13}C is hyperfine coupled to the NV^- center, yielding the system Hamiltonian ($\hbar=1$)

$$H_0 = DS_z^2 + \gamma_e S_z (B_z + B) + \gamma_c I_z (B_z + B) + S_z A_{zz} I_z, \quad (4)$$

where $D/2\pi = 2.87$ GHz is the zero-field splitting of the NV^- center, $\gamma_e/2\pi \approx 2.8$ MHz/G, and $\gamma_c/2\pi \approx 1.07$ kHz/G are the gyromagnetic ratios of the electron and ^{13}C nuclear spins, respectively. B is the small magnetic field to detect and A_{zz} is the hyperfine coupling strength. We choose a weakly coupled ^{13}C nuclear spin aligned close to the N-V axis, such that its anisotropic hyperfine coupling terms such as A_{zx} are small and thus neglected here.

To further simplify the analysis, we focus on the 2-level submanifold $\{|0\rangle(m_s = 0), |1\rangle(m_s = -1)\}$ for the electronic spin of the NV^- , while for the ^{13}C we consider the complete basis $|\uparrow\rangle$ ($m_I^c = +1/2$) and $|\downarrow\rangle$ ($m_I^c = -1/2$). In Fig. 1-(b) we show the energy levels of our configuration, indicating the relevant transitions with blue solid lines.

In order to manipulate the energy sublevels depicted in Fig. 1-(b), we apply a series of microwave (MW) and radiofrequency (RF) pulse sequences (square pulses) that results in the total Hamiltonian in a multi-rotating frame

$$\tilde{H} = \frac{1}{2} \begin{pmatrix} -\gamma_c B & \Omega_0^c & \Omega_\downarrow^c & 0 \\ \Omega_0^e & \gamma_c B & 0 & \Omega_\uparrow^e \\ \Omega_\downarrow^e & 0 & 2\delta_\downarrow^\downarrow & 0 \\ 0 & \Omega_\uparrow^e & 0 & 2\delta_\uparrow^\uparrow \end{pmatrix}, \quad (5)$$

where Ω_i^e and Ω_0^c are the Rabi frequencies of the MW and RF fields acting on the electron and nuclear spins,

respectively. $\delta_1^\uparrow = -\gamma_e B + \gamma_c B/2 - A_{zz}/2$ and $\delta_1^\downarrow = -\gamma_e B - \gamma_c B/2 + A_{zz}/2 + \Delta$, with Δ the MW detuning from the electron spin resonance.

In what follows, we apply our protocol (Fig. 1-(c)) to the system, which leads to the enhancement of the magnetic field sensitivity. First, the system is initialized to the state $|\Psi_i\rangle = |0\rangle \otimes |\downarrow\rangle$. Efficient nuclear spin initialization has been demonstrated in Refs. [39–43]. Second, we prepare the ^{13}C nuclear spin in a coherent superposition state $|0\rangle \otimes (\cos(\alpha/2)|\uparrow\rangle + \sin(\alpha/2)|\downarrow\rangle)$ via the RF field (Ω_0^c). Third, a strong MW pulse rotates the NV^- electronic spin by an angle θ_i which is independent of the ^{13}C nuclear spin state, yielding

$$|\Psi_{pre}\rangle = (\cos(\theta_i/2)|1\rangle + \sin(\theta_i/2)|0\rangle) \otimes (\cos(\alpha/2)|\uparrow\rangle + \sin(\alpha/2)|\downarrow\rangle). \quad (6)$$

We will refer to Eq. (6) as the pre-selected state and it serves two goals in the sensing protocol: firstly, it acquires a phase proportional to B , directly contributing to the magnetometry. Additionally, it enables a weak interaction between the ^{13}C and the NV^- that is fundamental for probabilistic quantum metrology and the enhancement of the sensitivity. Next step, we let the system evolve for an interrogation time τ , leading to

$$|\Psi_1\rangle = \cos(\theta_i/2) \cos(\alpha/2) e^{-i\delta_1^\uparrow \tau} |1\rangle \otimes |\uparrow\rangle + \cos(\theta_i/2) \sin(\alpha/2) e^{-i\delta_1^\uparrow \tau} |1\rangle \otimes |\downarrow\rangle + \sin(\theta_i/2) \cos(\alpha/2) e^{-i\gamma_c B \tau/2} |0\rangle \otimes |\uparrow\rangle + \sin(\theta_i/2) \sin(\alpha/2) e^{i\gamma_c B \tau/2} |0\rangle \otimes |\downarrow\rangle. \quad (7)$$

Finally the system is post-selected upon NV^- in a target state $|\psi_f\rangle = \cos(\theta_f/2)|1\rangle + \sin(\theta_f/2)|0\rangle$. This process is illustrated in Fig.1-(c). In sensing a weak magnetic field B , we have $\gamma_c B \tau \ll 1$. Therefore the post-selection leaves the nuclear spin in the state

$$|\bar{\phi}_{post}\rangle = \cos(\alpha/2) \cos(\theta_f/2) \cos(\theta_i/2) e^{-i\delta_1^\uparrow \tau} |\uparrow\rangle + \cos(\alpha/2) \sin(\theta_f/2) \sin(\theta_i/2) |\uparrow\rangle + \sin(\alpha/2) \cos(\theta_f/2) \cos(\theta_i/2) e^{-i\delta_1^\uparrow \tau} |\downarrow\rangle + \sin(\alpha/2) \sin(\theta_f/2) \sin(\theta_i/2) |\downarrow\rangle. \quad (8)$$

The above state needs to be normalized, such that $|\phi_{post}\rangle = |\bar{\phi}_{post}\rangle / \sqrt{P_s}$, where P_s is the probability of having a successful post-selection,

$$P_s = \frac{1}{2} (1 + \cos(\theta_f) \cos(\theta_i)) + \frac{\sin(\theta_f) \sin(\theta_i)}{2} \times \left(\cos^2(\alpha/2) \cos(\delta_1^\uparrow \tau) + \sin^2(\alpha/2) \cos(\delta_1^\downarrow \tau) \right). \quad (9)$$

The final signal is proportional to

$$\langle I_z \rangle = \frac{1}{4P_s} (1 + \cos(\theta_f) \cos(\theta_i)) \cos(\alpha) + \frac{\sin(\theta_f) \sin(\theta_i)}{2} \times \left(\cos^2(\alpha/2) \cos(\delta_1^\uparrow \tau) - \sin^2(\alpha/2) \cos(\delta_1^\downarrow \tau) \right). \quad (10)$$

At cryogenic temperature (4 K), the combination of single-shot readout (SSR) of the NV^- electron and a nuclear spin controlled CNOT gate on the electronic spin enables SSR of the nuclear spin to directly measure $\langle I_z \rangle$. SSR on the NV^- reaching $> 96\%$ fidelity takes $3.7 \mu\text{s}$ [44]. A nuclear spin controlled CNOT gate is in principle limited in speed only by the hyperfine interaction strength, which gives correspondingly a few to a few tens of microseconds [45, 48].

We now compare the signal obtained in Eq. (10) to the simple case of Ramsey spectroscopy $(\pi/2)_x - \tau - (\pi/2)_x$ considering a single spin, the NV^- electronic spin. The Ramsey signal follows $\langle S_z \rangle_R = 1/2 - \cos(\delta_1^\uparrow \tau)/2$. Notice that our protocol shares a common ground with the Ramsey technique when sensing DC magnetic field as phase sensing. Furthermore, when the nuclear spin related part is removed, our protocol converges to the conventional Ramsey sequence. Nevertheless, our protocol employs a more elaborate procedure involving the additional nuclear spin, allowing further gain in sensitivity via the post-selection process. To emphasize the role of post-selection, we analyze the case where no post-selection is carried out. Since $\langle I_z \rangle = \cos(\alpha)$ carries no information about the magnetic field in this case, we calculate the expectation value of I_x instead:

$$\langle I_x \rangle = \sin(\alpha) \left(\cos^2(\theta_i/2) \cos((\delta_1^\uparrow - \delta_1^\downarrow)\tau) + \sin^2(\theta_i/2) \right). \quad (11)$$

This brings no benefits as compared to the simpler case achieved with a single spin by the Ramsey sequence because the nuclear spin itself is not a very sensitive magnetometer. It is the post-selection that allows us to imprint the phase information into the nuclear spin, in such a way that variations of the post-selected angle θ_f calibrates the amount of information extracted from the measurement process [5].

IV. RESULTS

The magnetic field sensitivity is defined as the minimum detectable magnetic field normalized to a fixed interrogation (sensing) time [26]. The minimum detectable magnetic field is found through the standard deviation ΔB [28, 30],

$$\Delta B = \frac{\Delta I_z}{|\partial \langle I_z \rangle / \partial B|}, \quad (12)$$

where $\Delta I_z = \sqrt{\langle I_z^2 \rangle - \langle I_z \rangle^2}$ is the standard deviation of the signal from the ^{13}C nuclear spin.

Clearly, in order to increase the sensitivity, we need a fast variation of the signal $\langle I_z \rangle$ through the post-selection process. In Fig. 2-(a) we fix $B = 10^{-2}\text{G}$ and show the behavior of $\langle I_z \rangle$ as a function of the interrogation time τ . For convenience, we choose both spins initially prepared in a superposition state with $\alpha = \theta_i = \pi/2$ and the post-selected state to be parallel to the pre-selected electronic spin state $\theta_f = \pi/2$. Without loss of generality, we consider $A_{zz} = 100$ kHz and we set $\Delta = -0.56$ MHz to optimize the probability of post-selection and the standard deviation. Notice the region around $\tau = 7\mu\text{s}$ with a large slope of the signal, suggesting better sensitivity. The price to pay is a lower probability of successful post-selection (P_s), which reaches a minimum of 1.5%. This trade-off between the signal gain and the probability of success is common in protocols that rely on post-selection, as stated in the field of weak value amplification [2, 18]. Consequently, many trials are required for the successful post-selection. Interestingly, even when outcomes are discarded, there is valuable information in the post-selection's statistics that can be used [18, 23], given that P_s in Eq. (9) is a function of B .

Now we move on to show the minimum detectable field allowed in our protocol according to Eq. (12) in Fig. 2-(b). One observes from the plot that our protocol constitutes a better route towards minimizing ΔB in some parameter regimes. In other words, concentrating the most valuable information into a single successful measurement by post-selection provides an advantage for improving the minimum detectable magnetic field in a region in parameter space.

For practical purposes, a better witness to compare different sensing protocols is the sensitivity [26, 28, 30]

$$\eta = \Delta B \sqrt{t_m}, \quad (13)$$

where t_m is the total sequence time including initialization, interrogation and measurement. The initialization ($t_i = 20 \mu\text{s}$) and measurement time are usually fixed in a sequence, making the sensitivity dependent on the interrogation time. Moreover, the interrogation time τ is limited by dephasing of the magnetometer, given by the characteristic time T_2^* of the NV^- electronic spin. This is intuitive since the acquired phase will come together with the dephasing noise $\tilde{\varphi} = (-\gamma_e B - i/(2T_2^*))\tau$ and diminishes during interrogation. We split the measurement time for a single run into the post-selection time t_p (NV^- readout) and ^{13}C readout time t_r . Note that we have neglected some dead time used for control. Firstly, we focus on the low temperature regime, 4 K, where we can perform single-shot readout of the NV^- electronic spin ($t_p = 3.7 \mu\text{s}$ [44]) and ^{13}C nuclear spin ($t_r = 15 \mu\text{s}$ [48]). In Fig. 3, we show the sensitivity as a function of τ , for different coherence times, $T_2^* = \{100, 50, 10\} \mu\text{s}$. We consider a weak magnetic field $B = 10^{-2}$ G and $\alpha = \theta_i = \theta_f = \pi/2$. Note that as the coherence

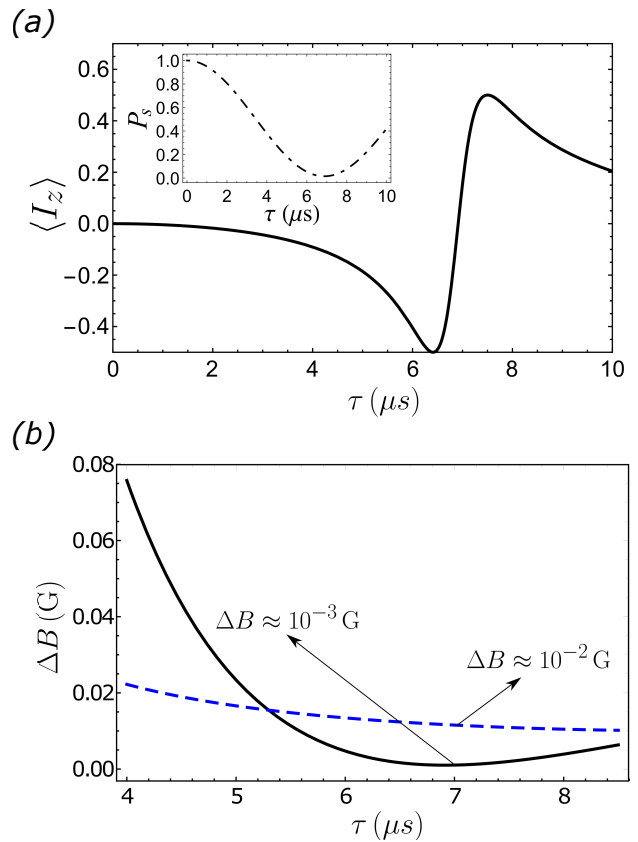


FIG. 2: (a) Varying the interrogation time τ we are able to strongly modify the nuclear spin signal $\langle I_z \rangle$. Note that around $\tau = 7 \mu\text{s}$ the signal becomes sharp, with a non-negligible probability of 5.4%. Parameters are $\alpha = \theta_i = \theta_f = \pi/2$, $B = 10^{-2}\text{G}$. (b) The standard deviation of the magnetic field ΔB obtained from the post-selection (black-solid) has been improved as compared with the one obtained from Ramsey spectroscopy (blue-dashed), allowing high precision measurements.

time given by T_2^* decreases, η increases, meaning that the sensitivity deteriorates. We numerically found that for T_2^* above $50 \mu\text{s}$ our protocol reaches a better sensitivity than the Ramsey sequence. However, below this interrogation time Ramsey sequence prevails. Although the T_2^* of naturally occurring NV^- electronic spins in a natural abundance diamond sample is typically around a few microseconds [15], it could be significantly increased in an isotopically purified sample [31]. It has been reported that in a 99.99% spinless ^{12}C diamond sample, a coherence time $T_2^* = 470 \pm 100 \mu\text{s}$ has been achieved [45], while about 10% of all NV^- still exhibits nearby ^{13}C 's. Therefore the parameter regime where a post-selection brings on practical advantages in sensitivity is achievable in experiment.

We emphasize that our protocol is versatile, and it can be coupled to another mechanism that improves the sensing part. First, recent works have paved the way to take advantage of the ^{13}C nuclear spin and use it as a memory to extend the interrogation time or refocus static

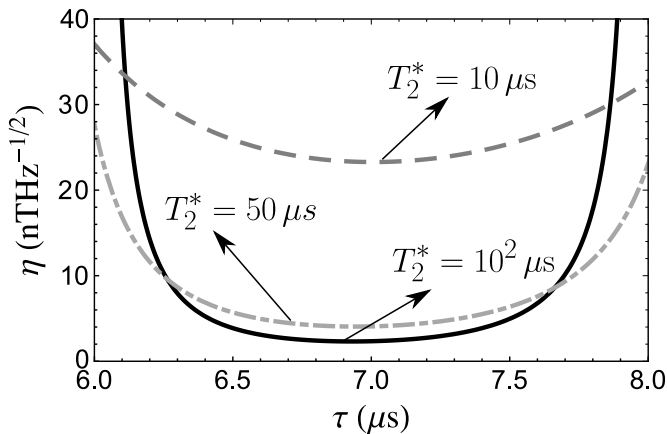


FIG. 3: Transverse relaxation deteriorates the protocol. As T_2^* decreases, η increases meaning that the sensitivity of the magnetometer decreases. Same parameters as in Fig. 2 and $t_m = 20 + \tau + 3.7 + 15 \mu s$.

noise [29, 46]. Second, one can apply active techniques to diminish the effect of the dephasing noise on the electronic spin, such as Continuous Driving with π -rotary-echo (RE) composite pulse [30], Continuous Dynamical Decoupling [32] or using error correction [47].

Hereafter, we consider an isotopically purified sample with the NV^- electron $T_2^* = 10^2 \mu s$. Moreover, there is a factor $C \leq 1$ [26, 27, 30], $\eta_C = \eta/C$, that takes into account readout inefficiencies (photon collection, contrast) and interactions with other elements in the diamond lattice. For our purified sample and assuming ideal single-shot readout, this factor approaches to unity. Therefore, we can roughly estimate the sensitivity of our magnetometer for an optimal interrogation time $\tau = 8.75 \mu s$ to be $\eta = 4.13 \text{ nTHz}^{-1/2}$ ($C = 1$), and for a non-ideal scenario ($C = 0.707$ [26]) we get $\eta_C = 5.84 \text{ nTHz}^{-1/2}$. We have set $\Delta = -0.30 \text{ MHz}$ to optimize the probability of success $P_s = 0.44$, which is a very high probability and doubles the typical values of experiments involving post-selection [14, 15].

At room temperature, the process is more challenging. Here, a high magnetic field is generally required ($B_z > 2000 \text{ G}$) [49] and also the presence of an auxiliary spin to perform repetitive readout. To accomplish this goal we consider the Nitrogen-14 nuclear spin (^{14}N),

and single-shot readout of electron is achieved by firstly mapping it to the ^{14}N and then readout the nuclear spin. Considering 2000 repetitions we obtain $t_p = 5 \text{ ms}$ [49] and $t_r = 30 \text{ ms}$ [48], leading to $\eta_C = 0.16 \mu\text{THz}^{-1/2}$.

V. CONCLUSIONS

In summary, we have presented a new experimentally feasible protocol based on post-selection to estimate a weak magnetic field. The information of the field is stored in a relative phase acquired by the electronic spin of a NV^- center in diamond during the weak interaction between the NV^- and a nearby ^{13}C nuclear spin. The most valuable information regarding the magnetic field is focused on a single successful measurement, a scenario that have been exploited in experiments with weak value amplification. By simulating realistic conditions of losses and readout inefficiencies, for coherence times above $T_2^* = 50 \mu s$ our sensitivity is better than the conventional Ramsey sequence, and at cryogenic temperature (4 K) we achieved few $\text{nTHz}^{-1/2}$, which is of the order of the theoretical attainable sensitivity for a single sensor spin [28]. In addition, at room temperature the most limiting factors are the slow control and the number of repetitions for the readout of the ^{13}C . The first can be further improved by considering a closer ^{13}C —assuming a coherence time that is long enough, or via stimulated Raman control [41]. The latter could be improved by using Bayesian estimation [50]. Finally, our protocol is suitable for decreasing the required interrogation time (τ) below the one needed for the same sensitivity with a Ramsey sequence, by appropriately choosing the parameter regime.

VI. ACKNOWLEDGMENTS

RC acknowledges support from Fondecyt Iniciación No. 11180143. H.T.D. acknowledges support from Fondecyt-postdoctorado Grant No. 3170922. AN acknowledges support from Universidad Mayor through the Postdoctoral fellowship. JRM acknowledges support from Fondecyt Regular No. 1180673 and AFOSR FA9550-18-1-0513.

-
- [1] B. M. Escher, R. L. de Matos Filho, and L. Davidovich. General framework for estimating the ultimate precision limit in noisy quantum-enhanced metrology. *Nature Physics*, 7(5):406–411, 2011.
- [2] Yakir Aharonov, David Z. Albert, and Lev Vaidman. How the result of a measurement of a component of the spin of a spin-1/2 particle can turn out to be 100. *Phys. Rev. Lett.*, 60:1351–1354, Apr 1988.
- [3] Justin Dressel, Mehul Malik, Filippo M. Miatto, An-

- drew N. Jordan, and Robert W. Boyd. Colloquium: Understanding quantum weak values: Basics and applications. *Rev. Mod. Phys.*, 86:307–316, Mar 2014.
- [4] Juan P. Torres and Luis José Salazar-Serrano. Weak value amplification: a view from quantum estimation theory that highlights what it is and what isn't. *Scientific Reports*, 6(1):19702, 2016.
- [5] Raul Coto, Víctor Montenegro, Vitalie Eremeev, Douglas Mundarain, and Miguel Orszag. The power of a

- control qubit in weak measurements. *Scientific Reports*, 7(1):6351, 2017.
- [6] Omar S Magaña-Loaiza, Jérémie Harris, Jeff S Lundeen, and Robert W Boyd. Weak-value measurements can outperform conventional measurements. *Physica Scripta*, 92(2):023001, dec 2016.
- [7] David R. M. Arvidsson-Shukur, Nicole Yunger Halpern, Hugo V. Lepage, Aleksander A. Lasek, Crispin H. W. Barnes, and Seth Lloyd. Quantum negativity provides advantage in postselected metrology, 2019.
- [8] N. W. M. Ritchie, J. G. Story, and Randall G. Hulet. Realization of a measurement of a “weak value”. *Phys. Rev. Lett.*, 66:1107–1110, Mar 1991.
- [9] G. J. Pryde, J. L. O’Brien, A. G. White, T. C. Ralph, and H. M. Wiseman. Measurement of quantum weak values of photon polarization. *Phys. Rev. Lett.*, 94:220405, Jun 2005.
- [10] P. Ben Dixon, David J. Starling, Andrew N. Jordan, and John C. Howell. Ultrasensitive beam deflection measurement via interferometric weak value amplification. *Phys. Rev. Lett.*, 102:173601, Apr 2009.
- [11] David J. Starling, P. Ben Dixon, Andrew N. Jordan, and John C. Howell. Optimizing the signal-to-noise ratio of a beam-deflection measurement with interferometric weak values. *Phys. Rev. A*, 80:041803, Oct 2009.
- [12] Nicolas Brunner and Christoph Simon. Measuring small longitudinal phase shifts: Weak measurements or standard interferometry? *Phys. Rev. Lett.*, 105:010405, Jul 2010.
- [13] Sacha Kocsis, Boris Braverman, Sylvain Ravets, Martin J. Stevens, Richard P. Mirin, L. Krister Shalm, and Aephraim M. Steinberg. Observing the average trajectories of single photons in a two-slit interferometer. *Science*, 332(6034):1170–1173, 2011.
- [14] Amir Feizpour, Xingxing Xing, and Aephraim M. Steinberg. Amplifying single-photon nonlinearity using weak measurements. *Phys. Rev. Lett.*, 107:133603, Sep 2011.
- [15] M. S. Blok, C. Bonato, M. L. Markham, D. J. Twitchen, V. V. Dobrovitski, and R. Hanson. Manipulating a qubit through the backaction of sequential partial measurements and real-time feedback. *Nature Physics*, 10(3):189–193, 2014.
- [16] Lijian Zhang, Animesh Datta, and Ian A. Walmsley. Precision metrology using weak measurements. *Phys. Rev. Lett.*, 114:210801, May 2015.
- [17] G. Bié Alves, A. Pimentel, M. Hor-Meyll, S. P. Walborn, L. Davidovich, and R. L. de Matos Filho. Achieving metrological precision limits through postselection. *Phys. Rev. A*, 95:012104, Jan 2017.
- [18] Joshua Combes, Christopher Ferrie, Zhang Jiang, and Carlton M. Caves. Quantum limits on postselected, probabilistic quantum metrology. *Phys. Rev. A*, 89:052117, May 2014.
- [19] George C. Knee, G. Andrew D. Briggs, Simon C. Benjamin, and Erik M. Gauger. Quantum sensors based on weak-value amplification cannot overcome decoherence. *Phys. Rev. A*, 87:012115, Jan 2013.
- [20] George C. Knee and Erik M. Gauger. When amplification with weak values fails to suppress technical noise. *Phys. Rev. X*, 4:011032, Mar 2014.
- [21] Christopher Ferrie and Joshua Combes. Weak value amplification is suboptimal for estimation and detection. *Phys. Rev. Lett.*, 112:040406, Jan 2014.
- [22] Saki Tanaka and Naoki Yamamoto. Information amplification via postselection: A parameter-estimation perspective. *Phys. Rev. A*, 88:042116, Oct 2013.
- [23] G. Bié Alves, B. M. Escher, R. L. de Matos Filho, N. Zagury, and L. Davidovich. Weak-value amplification as an optimal metrological protocol. *Phys. Rev. A*, 91:062107, Jun 2015.
- [24] Jennifer M. Schloss, John F. Barry, Matthew J. Turner, and Ronald L. Walsworth. Simultaneous broadband vector magnetometry using solid-state spins. *Phys. Rev. Applied*, 10:034044, Sep 2018.
- [25] K. Arai, J. Lee, C. Belthangady, D. R. Glenn, H. Zhang, and R. L. Walsworth. Geometric phase magnetometry using a solid-state spin. *Nature Communications*, 9(1):4996, 2018.
- [26] C. L. Degen, F. Reinhard, and P. Cappellaro. Quantum sensing. *Rev. Mod. Phys.*, 89:035002, July 2017.
- [27] J. M. Taylor, P. Cappellaro, L. Childress, L. Jiang, D. Budker, P. R. Hemmer, A. Yacoby, R. Walsworth, and M. D. Lukin. High-sensitivity diamond magnetometer with nanoscale resolution. *Nat. Phys.*, 4(10):810–816, 2008.
- [28] J. R. Maze, P. L. Stanwix, J. S. Hodges, S. Hong, J. M. Taylor, P. Cappellaro, L. Jiang, A.S. Zibrov, A. Yacoby, R. Walsworth, and M. D. Lukin. Nanoscale magnetic sensing with an individual electronic spin qubit in diamond. *Nature*, 455:644–647, 2008.
- [29] Sebastian Zaiser, Torsten Rendler, Ingmar Jakobi, Thomas Wolf, Sang-Yun Lee, Samuel Wagner, Ville Bergholm, Thomas Schulte-Herbruggen, Philipp Neumann, and Jorg Wrachtrup. Enhancing quantum sensing sensitivity by a quantum memory. *Nat. Commun.*, 7:–, August 2016.
- [30] Clarice D. Aiello, Masashi Hirose, and Paola Cappellaro. Composite-pulse magnetometry with a solid-state quantum sensor. *Nat. Commun.*, 4:1419–, Jan 2013.
- [31] Gopalakrishnan Balasubramanian, Philipp Neumann, Daniel Twitchen, Matthew Markham, Roman Kolesov, Norikazu Mizuochi, Junichi Isoya, Jocelyn Achard, Johannes Beck, Julia Tissler, Vincent Jacques, Philip R. Hemmer, Fedor Jelezko, and Jorg Wrachtrup. Ultralong spin coherence time in isotopically engineered diamond. *Nat. Mater.*, 8(5):383–387, 2009.
- [32] Masashi Hirose, Clarice D. Aiello, and Paola Cappellaro. Continuous dynamical decoupling magnetometry. *Phys. Rev. A*, 86:062320, Dec 2012.
- [33] I. Lovchinsky, A. O. Sushkov, E. Urbach, N. P. de Leon, S. Choi, K. De Greve, R. Evans, R. Gertner, E. Bersin, C. Müller, L. McGuinness, F. Jelezko, R. L. Walsworth, H. Park, and M. D. Lukin. Nuclear magnetic resonance detection and spectroscopy of single proteins using quantum logic. *Science*, 351(6275):836–841, 2016.
- [34] D.R. Glenn, D.B. Bucher, J. Lee, M.D. Lukin, H. Park, and R.L. Walsworth. High-resolution magnetic resonance spectroscopy using a solid-state spin sensor. *Nature*, 555(7696):351–354, 2018.
- [35] O. Sushkov, A., I. Lovchinsky, N. Chisholm, L. Walsworth, R., H. Park, and D. Lukin, M. Magnetic resonance detection of individual proton spins using quantum reporters. *Phys. Rev. Lett.*, 113:197601, Nov 2014.
- [36] Fazhan Shi, Qi Zhang, Pengfei Wang, Hongbin Sun, Jiarong Wang, Xing Rong, Ming Chen, Chenyong Ju, Friedemann Reinhard, Hongwei Chen, Jörg Wrachtrup, Junfeng Wang, and Jiangfeng Du. Single-protein spin

- resonance spectroscopy under ambient conditions. *Science*, 347(6226):1135–1138, 2015.
- [37] M. H. Abobeih, J. Randall, C. E. Bradley, H. P. Bartling, M. A. Bakker, M. J. Degen, M. Markham, D. J. Twitchen, and T. H. Taminiau. Atomic-scale imaging of a 27-nuclear-spin cluster using a quantum sensor. *Nature*, 576(7787):411–415, 2019.
- [38] Shengjun Wu and Klaus Mlmer. Weak measurements with a qubit meter. *Physics Letters A*, 374(1):34 – 39, 2009.
- [39] H.T. Taminiau, J. Cramer, T. van der Sar, V.V. Dobrovitski, and R. Hanson. Universal control and error correction in multi-qubit spin registers in diamond. *Nat Nano*, 9(3):171–176, March 2014.
- [40] P. Jamonneau, G. Hétet, A. Dréau, J.-F. Roch, and V. Jacques. Coherent population trapping of a single nuclear spin under ambient conditions. *Phys. Rev. Lett.*, 116:043603, Jan 2016.
- [41] Raul Coto, Vincent Jacques, Gabriel Hétet, and Jerónimo R. Maze. Stimulated raman adiabatic control of a nuclear spin in diamond. *Phys. Rev. B*, 96:085420, Aug 2017.
- [42] Jiwon Yun, Kiho Kim, and Dohun Kim. Strong polarization of individual nuclear spins weakly coupled to nitrogen-vacancy color centers in diamond. *New Journal of Physics*, 21(9):093065, sep 2019.
- [43] C. E. Bradley, J. Randall, M. H. Abobeih, R. C. Berrevoets, M. J. Degen, M. A. Bakker, M. Markham, D. J. Twitchen, and T. H. Taminiau. A ten-qubit solid-state spin register with quantum memory up to one minute. *Phys. Rev. X*, 9:031045, Sep 2019.
- [44] B. Hensen, H. Bernien, A. E. Dreau, A. Reiserer, N. Kalb, M. S. Blok, J. Ruitenber, R. F. L. Vermeulen, R. N. Schouten, C. Abellan, W. Amaya, V. Pruneri, M. W. Mitchell, M. Markham, D. J. Twitchen, D. Elkouss, S. Wehner, T. H. Taminiau, and R. Hanson. Loophole-free bell inequality violation using electron spins separated by 1.3 kilometres. *Nature*, 526(7575):682–686, October 2015.
- [45] P. C. Maurer, G. Kucsko, C. Latta, L. Jiang, N. Y. Yao, S. D. Bennett, F. Pastawski, D. Hunger, N. Chisholm, M. Markham, D. J. Twitchen, J. I. Cirac, and M. D. Lukin. Room-temperature quantum bit memory exceeding one second. *Science*, 336(6086):1283–1286, 2012.
- [46] Yuichiro Matsuzaki, Takaaki Shimo-Oka, Hirotaka Tanaka, Yasuhiro Tokura, Kouichi Semba, and Norikazu Mizuochi. Hybrid quantum magnetic-field sensor with an electron spin and a nuclear spin in diamond. *Phys. Rev. A*, 94:052330, Nov 2016.
- [47] Sisi Zhou, Mengzhen Zhang, John Preskill, and Liang Jiang. Achieving the heisenberg limit in quantum metrology using quantum error correction. *Nature Communications*, 9(1):78, 2018.
- [48] A. Dréau, P. Spinicelli, J. R. Maze, J.-F. Roch, and V. Jacques. Single-shot readout of multiple nuclear spin qubits in diamond under ambient conditions. *Phys. Rev. Lett.*, 110:060502, Feb 2013.
- [49] Philipp Neumann, Johannes Beck, Matthias Steiner, Florian Rempp, Helmut Fedder, Philip R. Hemmer, Jorg Wrachtrup, and Fedor Jelezko. Single-shot readout of a single nuclear spin. *Science*, 5991:542–544, 2010.
- [50] Hossein T. Dinani, Dominic W. Berry, Raul Gonzalez, Jeronimo R. Maze, and Cristian Bonato. Bayesian estimation for quantum sensing in the absence of single-shot detection *Phys. Rev. B*, 99:125413, 2019.